Mesenchymal Stromal Cell-Derived PTX3 Promotes Wound Healing via Fibrin Remodeling

Claudia Cappuzzello[1], Andrea Doni[2], Erica Dander[1], Fabio Pasqualini[2], Manuela Nebuloni[3], Barbara Bottazzi[2], Alberto Mantovani[2], Andrea Biondi[1], Cecilia Garlanda[2] and Giovanna D'Amico[1]

Although mesenchymal stromal cells (MSCs) can promote wound healing in different clinical settings, the underlying mechanism of MSC-mediated tissue repair has yet to be determined. Because a nonredundant role of pentraxin 3 (PTX3) in tissue repair and remodeling has been recently described, here we sought to determine whether MSC-derived PTX3 might play a role in wound healing. Using a murine model of skin repair, we found that *Ptx3*-deficient ($Ptx3^{-/-}$) MSCs delayed wound closure and reduced granulation tissue formation compared with wt MSCs. At day 2, confocal microscopy revealed a dramatic reduction in green fluorescent protein (GFP)-expressing $Ptx3^{-/-}$ MSCs recruited to the wound, where they appeared to be not only poorly organized in bundles but also scattered in the extracellular matrix. These findings were further confirmed by quantitative biochemical analysis of GFP content in wound extracts. Furthermore, $Ptx3^{-/-}$ MSC-treated skins displayed increased levels of fibrin and lower levels of D-dimer, suggesting delayed fibrin-rich matrix remodeling compared with control skins. Consistently, both pericellular fibrinolysis and migration through fibrin were found to be severely affected in $Ptx3^{-/-}$ MSCs. Overall, our findings identify an essential role of MSC-derived PTX3 in wound repair underscoring the beneficial potential of MSC-based therapy in the management of intractable wounds.

Journal of Investigative Dermatology (2016) **136,** 293-300; doi:10.1038/JID.2015.346

INTRODUCTION

Optimal wound healing requires a well-orchestrated integration of biological and molecular events regulating cell migration, proliferation, and extracellular matrix (ECM) remodeling (Martin, 1997; Singer and Clark, 1999). As wound healing impairment represents a major health problem, the cellular and molecular events required for appropriate repair constitute a major research focus. In this regard, the presence of mesenchymal stromal cells (MSCs) in both epidermal and dermal compartments (Sellheyer and Krahl, 2010; Toma et al., 2001), and their critical role in skin renewal (Badiavas et al., 2003) have prompted many investigators to utilize MSCs for the treatment of nonhealing wounds resulting from burns (Bey et al., 2010), diabetes (Falanga et al., 2007), and Crohn's disease (Ciccocioppo et al., 2011). Mounting evidence suggests that MSC paracrine signaling, rather than MSC differentiation, might constitute the main regulatory pathway involved in MSC-enhanced tissue repair (Hocking and Gibran, 2010; Liu et al., 2014). Nevertheless, the complex interactions of MSCs with their surrounding environment during wound healing and the signaling pathway mediating this process are not completely understood.

Pentraxin 3 (PTX3) is an essential component of the humoral arm of innate immunity (Bottazzi et al., 2010), involved in the resistance against microorganisms (Lu et al., 2008) and inflammation (Deban et al., 2010). It is well established that key activators of the inflammatory and reparative response after tissue injury, such as proinflammatory cytokines and Toll-like receptors, induce PTX3 production in different cell types, including stromal cells (Bottazzi et al., 2010; Dinarello, 2009; Medzhitov, 2008). Moreover, the secretome of adipose tissue–derived MSCs contains high levels of PTX3 during the early stages of mesengenic differentiation (Chiellini et al., 2008).

A more recent study has shown that PTX3 plays a nonredundant protective role in the regulation of tissue repair and remodeling (Doni et al., 2015). Doni et al. found that in acidic conditions occurring during tissue damage and repair, PTX3 bound fibrinogen and/or fibrin and plasminogen and increased plasmin-mediated pericellular fibrinolysis. In this regard, murine models of tissue damage showed a correlation between PTX3 deficiency and increased fibrin deposition and persistence followed by augmented collagen deposition. Furthermore, Ptx3-deficient remodeling cells showed alterations in the organization and migration throughout the provisional fibrin matrix. Interestingly, throughout the wound healing process, among other remodeling cells, stromal cells of mesenchymal origin appeared to be the major source of PTX3 (Doni et al., 2015).

On the basis of this initial characterization and the abovementioned findings, we sought to determine the functional

[1]*Centro Ricerca Tettamanti, Department of Pediatrics, University of Milano-Bicocca, Fondazione MBBM/San Gerardo Hospital, Monza, Italy;* [2]*IRCCS—Humanitas Clinical and Research Center, Rozzano, Milan, Italy; and* [3]*Pathology Unit, L. Sacco Department of Clinical Sciences, L. Sacco Hospital, Università degli Studi di Milano, Milan, Italy*

Correspondence: Giovanna D'Amico, Centro Ricerca Tettamanti, Fondazione MBBM/San Gerardo Hospital, via Pergolesi 33, 20900 Monza, Italy. E-mail: giovanna.damico@hsgerardo.org

Abbreviations: BM, bone marrow; ECM, extracellular matrix; MSCs, mesenchymal stromal cells; PTX3, pentraxin 3; $Ptx3^{-/-}$, Ptx3-deficient

Received 28 April 2015; revised 5 August 2015; accepted 12 August 2015; accepted manuscript published online 3 September 2015

role of PTX3 during tissue repair and remodeling exerted by bone marrow (BM)-derived MSCs. For this purpose, we analyzed the effect of *Ptx3*-deficient ($Ptx3^{-/-}$) MSCs on a murine model of excisional cutaneous wound healing.

To our knowledge, this study describes a previously unreported mechanism of MSC-derived PTX3 in wound closure, underscoring the therapeutic potential of MSCs-based strategies in the treatment of nonhealing wounds.

RESULTS

In vitro characterization of BM-derived $Ptx3^{-/-}$ and wt MSCs

We first evaluated basal or cytokine-induced PTX3 production in the supernatants of wt MSCs by ELISA. As shown in Figure 1a, detectable levels of PTX3 were found in the culture medium of unstimulated MSCs (0.22 ± 0.13 ng/ml of protein; mean ± SEM; n = 4). Exposure of MSCs to IL-1β, tumor necrosis factor-α, and IL-6 for 24 hours led to a robust induction of PTX3 protein expression in the supernatant (33.34 ± 11.68 ng/ml of protein; mean ± SEM, compared with unexposed MSCs). As expected, the expression of PTX3 was undetectable in both unexposed and cytokine-stimulated $Ptx3^{-/-}$ MSCs, as shown in Figure 1b.

To investigate the role of PTX3 in MSC-mediated wound healing, we isolated $Ptx3^{-/-}$ MSCs from BM of *Ptx3* knockout mice and extensively characterized them for their phenotypical and functional properties before using them in vivo. Both $Ptx3^{-/-}$ and wt MSCs were found to be strongly positive for stromal cell–associated antigens such as CD29, CD90, and ScaI, and negative for hematopoietic myeloid and lymphoid markers, as assessed by FACS analysis (Figure 1c). When cultured in adipogenic and osteogenic medium, both $Ptx3^{-/-}$ *and* wt MSCs differentiated into adipocytes and osteoblasts (Figure 1d).

Next, we sought to determine the spontaneous (unstimulated) proliferation of both $Ptx3^{-/-}$ and wt MSC lines. We

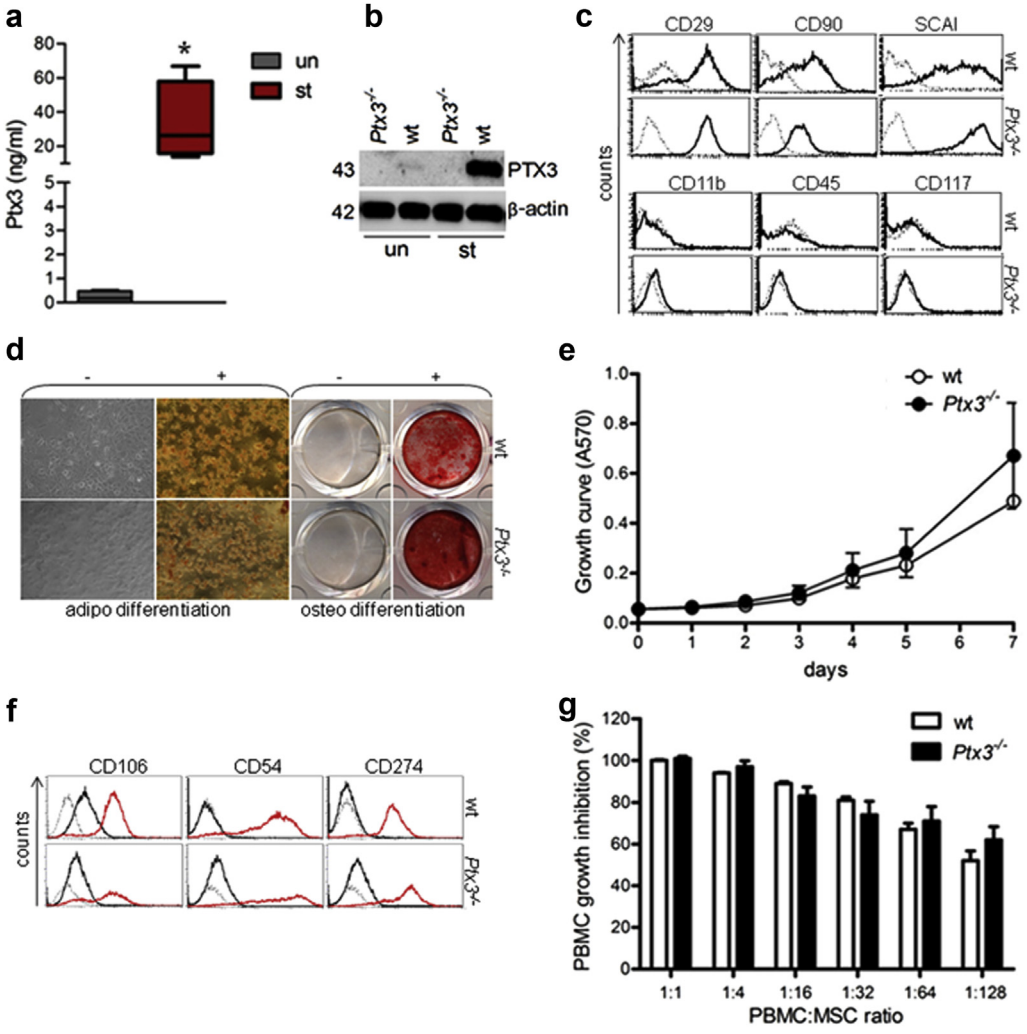

Figure 1. In vitro characterization of BM-derived $Ptx3^{-/-}$ and wt MSCs. (**a**) Box plot showing the PTX3 content in supernatants (n = 4) of cytokine-stimulated (st) wt MSCs. *$P \leq 0.05$, versus unexposed MSCs (un). (**b**) PTX3 deficiency in $Ptx3^{-/-}$ MSCs and increased expression in the wt MSCs on cytokine exposure. (**c**) Representative FACS analysis (n = 3) of $Ptx3^{-/-}$ and wt MSCs (dotted line, control; black line, cells with antibody). (**d**) Microscopic view showing the lipid drop accumulation (left panel; Oil Red-O staining) and mineralization (right panel; Alizarin Red-S staining) after 3 weeks of culture in control (−) and induction medium (+). (**e**) Unstimulated MSC proliferation. (**f**) Expression of CD106, CD54, and CD274 after 24 hours of stimulation with IFN-γ and TNF-α. Black or red line: antigen expression of unstimulated or stimulated MSC, respectively; black-dotted line, isotype Ab. (**g**) Inhibition of lymphocyte proliferation by MSCs. BM, bone marrow; MSC, mesenchymal stromal cell; PTX3, pentraxin 3; $Ptx3^{-/-}$, *Ptx3*-deficient; TNF-α, tumor necrosis factor-α.

found that the growth rate of *Ptx3*$^{-/-}$ MSCs (n = 3) did not differ significantly from that of wt MSCs (n = 3) throughout the entire time course, as assessed by the 3-[4,5-dimethylthiazol-2-yl]-2,5-diphenyltetrazolium bromide (MTT) assay (Figure 1e). Furthermore, we determined the expression of molecules involved in the immunomodulatory properties of MSCs by FACS analysis. On 24 hours of tumor necrosis factor-α and IFN-γ treatment, both *Ptx3*$^{-/-}$ and wt MSCs displayed similar patterns of expression levels of adhesion molecules, such as CD106/VCAM-1 and CD54/ICAM-1, as well as CD274/programmed death ligand-1 (Figure 1f).

Finally, we assessed the ability of *Ptx3*$^{-/-}$ MSCs to affect lymphocyte proliferation induced by phytohemagglutinin. As shown in Figure 1g, *Ptx3*$^{-/-}$ MSCs (n = 4) inhibited lymphocyte proliferation in a dose-dependent manner similarly to wt MSCs (n = 4).

PTX3 deficiency in MSCs affects skin wound healing

To examine the effect of PTX3 deficiency in MSCs on wound closure, mice were wounded on the back and immediately treated with *Ptx3*$^{-/-}$ or wt MSCs. The analysis of wound closure kinetics revealed that, consistent with previous studies (Javazon et al., 2007; Sasaki et al., 2008; Wu et al., 2007), wt MSCs increased the percentage of wound closure (52.01 ± 1.7 vs. 23.6 ± 5.07; values represent mean ± SEM percentage wound closure by wt MSC-treated vs. vehicle-treated wounds, respectively, at day 3 after wound creation) (Figure 2a and b). In contrast, *Ptx3*$^{-/-}$ MSCs showed impaired ability to accelerate wound closure compared with wt cells throughout the entire time course ($P \leq 0.01$ up to day 9 and $P \leq 0.05$ from day 10 to day 14) (Figure 2a and b). Furthermore, *Ptx3*$^{-/-}$ MSCs failed to enhance wound closure versus sham since day 2 up to day 9 after wounding, and only a minor effect was observed on days 10 and 11 ($P \leq 0.05$ at days 10 and 11).

To perform histological or immunohistochemical staining, wounds with surrounding skin were excised from both MSC-treated and sham mice. At day 7 after wounding, computer-assisted morphometric analysis of hematoxylin and eosin staining revealed a severe reduction of the granulation tissue area in wounds treated with *Ptx3*$^{-/-}$ MSCs (5.4 ± 0.56 vs. 8.0 ± 0.99 mm^2; values represent the mean ± SEM granulation tissue area of *Ptx3*$^{-/-}$ MSCs- vs. wt MSCs-treated wounds) (Figure 2c and d). Furthermore, as PTX3 modulates the inflammatory response (Deban et al., 2010), we quantified the immune cell subpopulations recruited to the wound bed of MSC-treated and vehicle-treated skins. Throughout the wound healing process, we did not observe any difference in recruitment of both granulocytes (GR-1$^+$ cells) and macrophages and/or monocytes (F4/80$^+$ cells) (data not shown). Similarly, capillary density, assessed by CD31 staining at 2, 7, and 14 days after wounding, did not differ among groups (data not shown).

Defective recruitment of *Ptx3*$^{-/-}$ MSCs at the wound site

To ascertain whether the impaired healing capacity of *Ptx3*$^{-/-}$ MSCs was attributable to their defective recruitment to the sites of injury, we analyzed the amount of these cells in the wound bed at day 2 after wounding. To this end, a new set of wound healing experiments were performed treating the wounds with GFP-expressing (GFP$^+$) MSCs or vehicle alone (sham). Subsequently, GFP$^+$ MSC distribution in wound sections, as well as PTX3 expression, was determined by confocal microscopy. As shown in Figure 3a, numerous GFP$^+$ wt MSCs were detected in the entire wound area at day 2. These cells were organized in aligned bundles that collectively invaded the wound bed and the

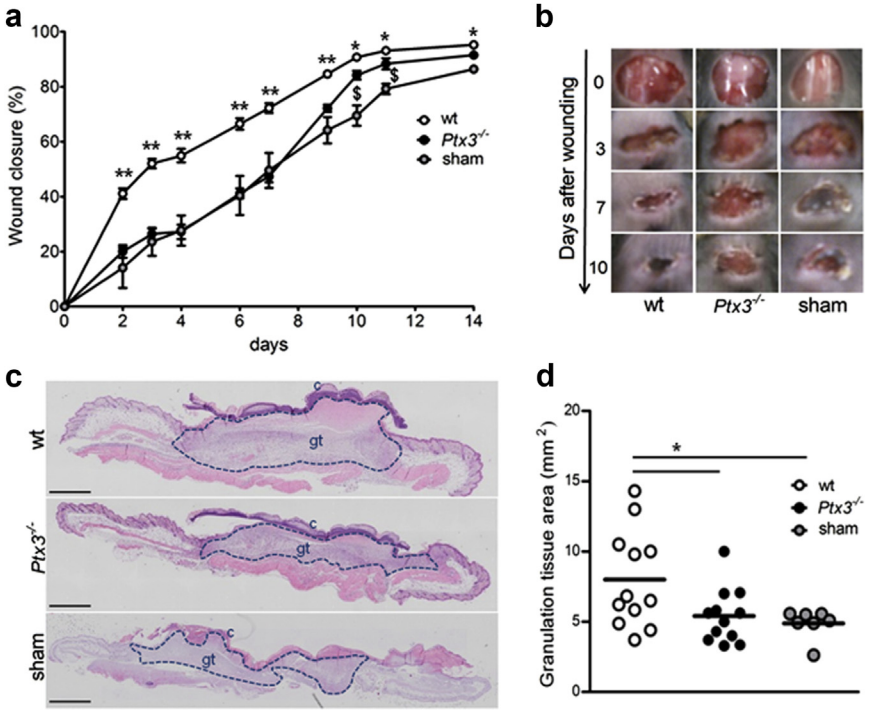

Figure 2. Effect of *Ptx3*$^{-/-}$ MSCs on wound healing. (**a**) Kinetics of excisional wound closure in mice treated with *Ptx3*$^{-/-}$ (n = 33), wt MSCs (n = 45) and vehicle (sham) (n = 15), respectively. Values represent the mean percentage of wound closure ± SEM (n = 5 experiments), $^{**}P \leq 0.01$, and $^{*}P \leq 0.05$, *Ptx3*$^{-/-}$ versus wt MSCs. $\$P \leq 0.05$, *Ptx3*$^{-/-}$ MSCs versus sham. (**b**) Representative digital photographs of full-thickness excisional wounds taken immediately or at different time points after wounding. (**c**) Representative photographs of histology at day 7 (×20 magnification). c, clot; gt, granulation tissue. Bar = 1,000 μm. (**d**) Graph showing computer-assisted morphometrical analysis of the granulation tissue area (from 7 to 12 samples analyzed) at day 7. $^{*}P \leq 0.05$, *Ptx3*$^{-/-}$ MSCs versus wt MSCs or wt MSCs versus sham. MSC, mesenchymal stromal cell; *Ptx3*$^{-/-}$, *Ptx3*-deficient.

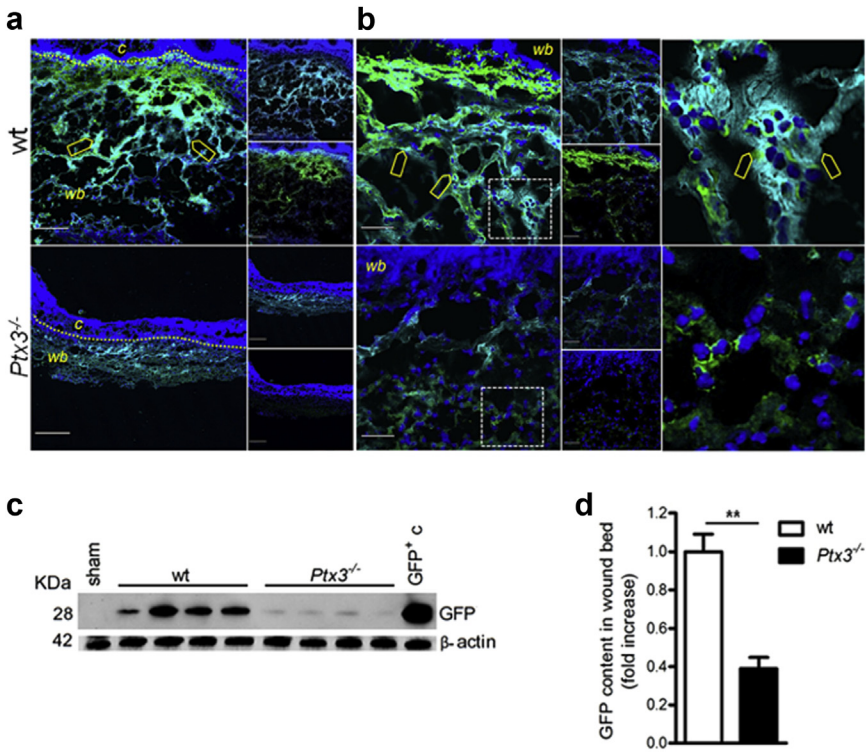

Figure 3. Analysis of *Ptx3*$^{-/-}$ MSC recruitment to the wounded skin and colocalization of PTX3 expression with the pericellular matrix of MSCs. (**a**, **b**) Confocal images of wt (n = 5) and *Ptx3*$^{-/-}$ (n = 5) MSCs entering the clot (c) and wound bed (wb) (day 2). (**a**) ×10; (**b**) ×40. (**a**, **b**) left panels: merged images; right panels: staining of nucleus (blue, upper and lower panels) and PTX3 (cyan, upper panel), or nucleus and GFP (green, lower panel). Yellow arrowheads: localization of PTX3 at the pericellular matrix of MSCs invading the wound bed. (**b**) right: close-up of squared areas in (**b**) left. Bar = 200 μm (**a**) or 50 μm (**b**). (**c**) Western blotting and (**d**) densitometry of GFP and β-actin expression in wound extracts (day 2). Data are fold change mean ± SEM of four independent samples. Lysates from 1 sham wound and GFP^{+} cells (**c**) were loaded as controls. $^{**}P \leq 0.01$, versus wt MSCs. GFP, green fluorescent protein; MSC, mesenchymal stromal cell; PTX3, pentraxin 3; *Ptx3*$^{-/-}$, *Ptx3*-deficient.

clot area. High levels of PTX3 protein expression were also found to be colocalized with the pericellular matrix of MSCs (Figure 3b). In contrast, fewer GFP^{+} *Ptx3*$^{-/-}$ MSCs were found in the wound bed (Figure 3a and b). Interestingly, these cells, which were not associated with PTX3 expression, appeared to be not only poorly organized in bundles but also scattered in the ECM (Figure 3a and b). As expected, much lower PTX3 expression levels were detected in these skin specimens compared with control (Figure 3a and b).

The evidence from the confocal microscopy was strongly supported by the quantitative biochemical analysis of GFP content in wound extracts. Western blot analysis of wound lysates showed that skins that had been treated with *Ptx3*$^{-/-}$ MSCs contained significantly lesser GFP than those treated with control cells (0.38 ± 0.05; fold increase ± SEM over wt MSC-treated skins), indicating a dramatic reduction in recruited *Ptx3*$^{-/-}$ MSCs at day 2 (Figure 3c and d).

Impaired pericellular fibrinolysis in *Ptx3*$^{-/-}$ MSCs

Previously, PTX3 has been shown to interact with provisional matrix components, fibrinogen and/or fibrin, and plasminogen deposited after injury and to facilitate fibrin dissolution (Doni et al., 2015). Thus, we sought to determine whether this function might be altered in our animal model. For this purpose, we employed confocal microscopy to analyze the fibrin-rich matrix that filled the wound bed of MSC-treated wounds and simultaneously localize PTX3 immunostaining. At day 2, we observed a very loose fibrin matrix in the skins treated with wt MSCs. In these samples, PTX3 colocalized with fibrin fibers and with the ECM of numerous cells invading the wound bed (Figure 4a). In contrast, more abundant and dense fibrin matrix and lower levels of associated PTX3 were detected in *Ptx3*$^{-/-}$ MSC-treated wounds (Figure 4a). Computer-assisted fluorescence analysis of fibrin in the wound bed of five specimens per group revealed increased fibrin deposition in *Ptx3*$^{-/-}$ MSC-treated wounds compared with control wounds (Figure 4b).

To determine fibrin-clot degradation, we measured soluble fibrinolysis products in wound extracts at day 2 after wounding. We found a significant decrease in the total amount of D-dimer, a product derived from fibrinogen, in wounds treated with *Ptx3*$^{-/-}$ MSCs compared with wt MSCs (76.07 ± 7.59 vs. 110.85 ± 7.09 pg protein; mean ± SEM, respectively) (Figure 4c), indicating delayed fibrinogen degradation and impaired clot remodeling in wounds exposed to *Ptx3*$^{-/-}$ MSCs.

Next, we assessed the pericellular fibrinolysis of *Ptx3*$^{-/-}$ and wt MSCs. Because PTX3 has been recently shown to potentiate the fibrinolysis mediated by plasmin and triggered by the urokinase-type plasminogen activator (Doni et al., 2015), we sought to determine whether the impairment of plasmin-mediated signaling could affect the fibrinolytic capacity of MSCs. For this purpose, *Ptx3*$^{-/-}$ and wt MSCs were embedded in fibrin gel and their ability to induce fibrinolysis was examined in the presence or absence of the two plasminogen-conversion inhibitors aprotinin and plasminogen activator inhibitor-1. After 36 hours of culture, *Ptx3*$^{-/-}$ MSCs showed a significantly reduced ability to digest the fibrin clot compared with wt cells (Figure 5a and b). This result was quantified by measuring the amount of soluble fibrinolysis-derived products in the culture medium of *Ptx3*$^{-/-}$ and wt MSCs by ELISA (Figure 5a), and visualized by SDS-PAGE (Figure 5b). The decrease in fibrinolysis was not attributable to a decreased proliferation rate of *Ptx3*$^{-/-}$ MSCs because there was no significant difference between wt and *Ptx3*$^{-/-}$ MSC total cell count (data not shown). Furthermore, fibrinolysis of MSCs was drastically abolished by the serine

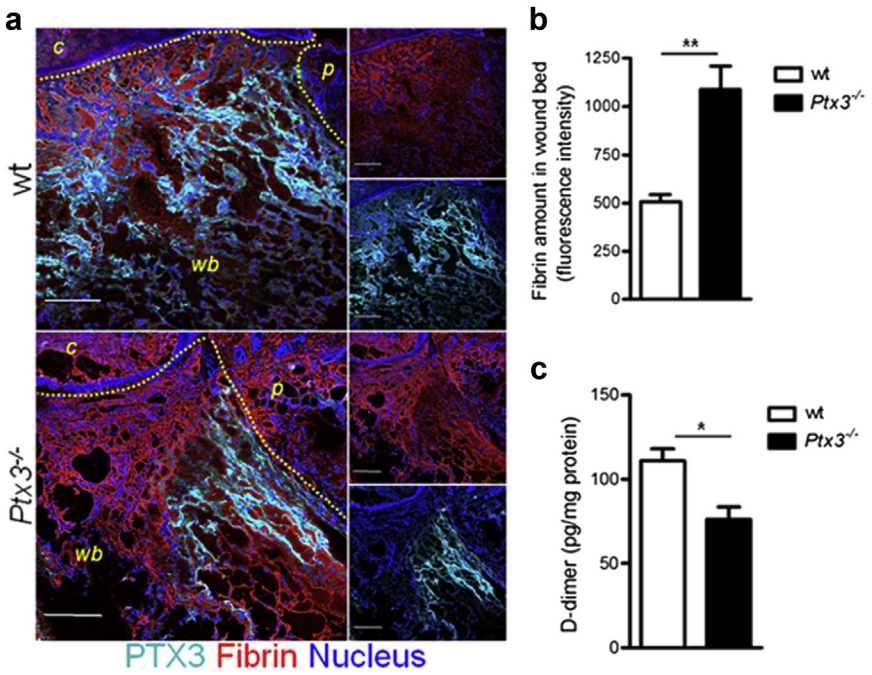

Figure 4. Fibrin-rich matrix remodeling in wounds treated with *Ptx3*$^{-/-}$ MSCs. (**a**) Representative confocal images (×10) of day 2 skin specimens (n = 5), showing fibrin immunostaining (red) in the wound bed (wb), and colocalization of PTX3 (cyan) with fibrin fibers. Upper panel: bundles of PTX3-expressing cells invading the loose fibrin matrix of wounded skins treated with wt MSCs. Bottom panel: confluent fibrin staining in the matrix of *Ptx3*$^{-/-}$ MSC-treated wounds. Left panels: merged images; right panels: single markers with nucleus (blue) are shown. C, clot; p, perilesion area. Bar = 200 μm. (**b**) Fibrin staining quantification in the wound bed of *Ptx3*$^{-/-}$ and wt MSC-treated skins. $^{**}P \leq 0.01$, *Ptx3*$^{-/-}$ MSC- versus wt MSC-treated wounds. (**c**) ELISA of D-dimer content in wound extracts at day 2. $^{*}P \leq 0.05$, *Ptx3*$^{-/-}$ MSC versus wt MSC-treated wounds. MSC, mesenchymal stromal cell; PTX3, pentraxin 3; *Ptx3*$^{-/-}$, *Ptx3*-deficient.

protease inhibitors aprotinin and plasminogen activator inhibitor-1 (Figure 5a and b), indicating that a plasmin-mediated fibrinolysis mechanism occurred in our model.

Next, we analyzed whether PTX3 expression was required for MSC migration through fibrin in vitro. For this purpose, we tested the migratory abilities of *Ptx3*$^{-/-}$ and wt MSCs in response to CXCL12, which is an important regulator of stem cell recruitment (Liu et al., 2011; Son et al., 2006). As shown in Figure 6, both *Ptx3*$^{-/-}$ and control MSCs efficiently migrated toward CXCL12 on uncoated filters, with no statistically significant difference. However, *Ptx3*$^{-/-}$ MSCs displayed a significantly lower migration index through the fibrin compared with wt MSCs (0.83 ± 0.16 vs. 1.35 ± 0.09, migration index ± SEM), indicating an essential role of PTX3 in fibrin invasive capacity of MSCs.

DISCUSSION

In vivo studies have shown that the administration of MSCs to either acute or chronic wounds improves wound healing by increasing granulation tissue formation, accelerating re-epithelialization and stimulating angiogenesis (Alfaro et al., 2008; Chen et al., 2008; McFarlin et al., 2006; Sasaki et al., 2008; Wu et al., 2007). Here, using an animal model of excisional wound healing, we show that the repairing ability of MSCs is crucially dependent on PTX3 expression.

PTX3 is a prototypic component of the humoral arm of innate immunity secreted in response to inflammatory stimuli and during the wound healing process by different cell types, including stromal cells (Bottazzi et al., 2010; Doni et al., 2015). In this regard, here, we show that stimulation with inflammatory cytokines induces PTX3 expression in the culture medium of BM-derived MSCs.

Recently, Doni et al., in agreement with previous reports (Deban et al., 2010; Norata et al., 2009; Rodriguez-Grande et al., 2014; Salio et al., 2008), have shown a nonredundant protective role of PTX3 in the regulation of tissue repair and remodeling (Doni et al., 2015). PTX3 deficiency was associated with increased clotting, excessive fibrin accumulation, and delayed re-epithelialization at early time points, followed by augmented collagen deposition, epithelial hyperplasia, and defective mature tissue formation at healing. This phenotype was attributed to the lack of PTX3-dependent facilitated plasmin-mediated fibrinolysis by tissue remodeling cells, which is a prerequisite for appropriate tissue repair (Doni et al., 2015). In this respect, fibrin and other provisional ECM proteins are deposited after tissue injury and their subsequent timely degradation is essential for tissue repair (Carmeliet et al., 1994; de Giorgio-Miller et al., 2005).

On the basis of the above findings, in this study, we sought to determine whether the lack of PTX3 in BM-derived MSCs would similarly impair the tissue repair properties of MSCs during wound healing. On in vitro analysis, *Ptx3*$^{-/-}$ MSCs were similar to their wild-type counterpart in their ability to grow spontaneously, undergo mesengenic differentiation, and express MSC cell-surface antigens commonly found in mesenchymal stromal cells. Furthermore, the ability of *Ptx3*$^{-/-}$ MSCs to inhibit the proliferation of activated lymphocytes, as well as the expression of immunological markers, was identical to that of control MSCs. However, although treatment with wt MSCs enhanced wound repair activity in our allogenic murine model of skin repair, in good agreement with previous studies (Javazon et al., 2007; Sasaki et al., 2008; Wu et al., 2007), exposure to *Ptx3*$^{-/-}$ MSCs led to a significant delay in wound closure throughout the entire healing process. *Ptx3*$^{-/-}$ MSCs had no effect on the wound closure that was comparable to that seen in vehicle-treated mice up to day 9 after wounding. Nevertheless, a minor effect of *Ptx3*$^{-/-}$ MSCs, which needs further investigation, was observed when compared to vehicle in the last phase of the wound healing process. *Ptx3*$^{-/-}$ MSCs failed to be recruited to the wound bed already at day 2, because of their defective invasion and remodeling of fibrin clot. However, because

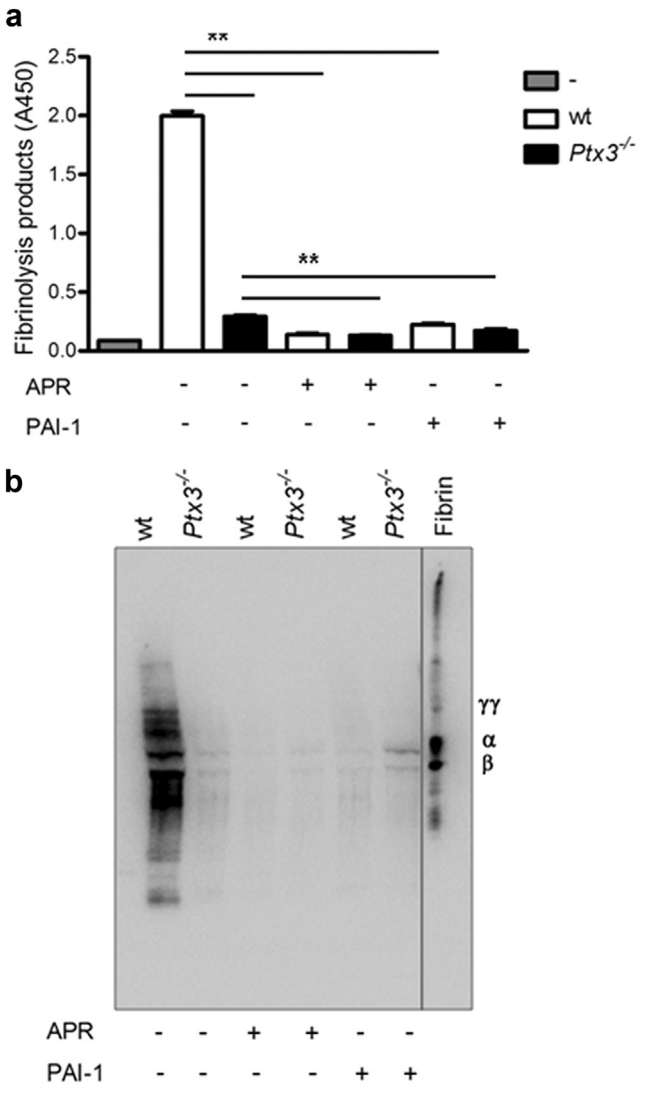

Figure 5. In vitro pericellular fibrinolysis of *Ptx3*$^{-/-}$ MSCs. (**a**) ELISA of soluble fibrinolysis products generated by *Ptx3*$^{-/-}$ and wt MSCs embedded in fibrin gel with or without APR or PAI-1. Values are expressed as O.D. mean ± SEM of triplicates. Gray column represents medium without cells. $^{**}P \leq 0.01$. (**b**) Western blot analysis showing the decreased amount of fibrinolysis products in culture of *Ptx3*$^{-/-}$ MSCs and the fibrinolysis abolishment by plasminogen-conversion inhibitors. Mouse serum (1 µl/lane) was also loaded. α, β, and γ chains of mouse fibrinogen are shown. APR, aprotinin; MSC, mesenchymal stromal cell; PAI-1, plasminogen activator inhibitor-1; PTX3, pentraxin 3; *Ptx3*$^{-/-}$, *Ptx3*-deficient.

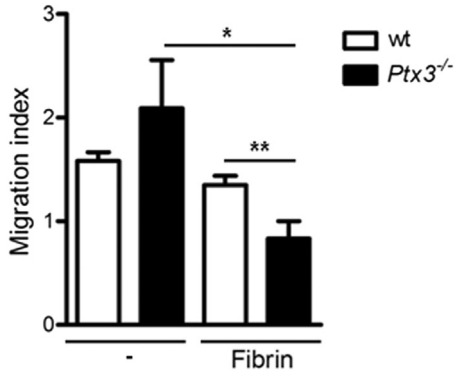

Figure 6. Migration of *Ptx3*$^{-/-}$ MSCs through fibrin. Migration ability of *Ptx3*$^{-/-}$ and wt MSCs (n = 2) through uncoated (–) or fibrin-coated filters in response to CXCL12 (200 ng/ml). Results are expressed as migration index ± SEM of stimulated versus unstimulated cells. The migration index was calculated as the ratio of the number of cells migrating toward the CXCL12 gradient to the number of cells migrating toward medium alone. Five-six randomly selected fields/insert were evaluated in three independent experiments. $^{**}P \leq 0.01$; $^{*}P \leq 0.05$. MSC, mesenchymal stromal cell; *Ptx3*$^{-/-}$, *Ptx3*-deficient.

Ptx3$^{-/-}$ MSCs have the same properties as their wt counterparts in terms of immunomodulatory capacities and differentiation potential, it is conceivable that soluble factor(s) secreted by *Ptx3*$^{-/-}$ MSCs in the perilesion area might have positively influenced, in a paracrine fashion, other resident cells responsible for the repair and/or remodeling such as endogenous fibroblasts and/or MSCs.

In our animal model, the most important morphological event that accompanied the impaired healing by *Ptx3*$^{-/-}$ MSCs was the reduction in the granulation tissue. Nevertheless, *Ptx3*$^{-/-}$ and wt MSC-treated wounds had similar capillary density during the healing, suggesting no difference in the angiogenesis promoted by the two MSC treatments. Likewise, as shown previously (Doni et al., 2015), we observed no difference in the number of recruited inflammatory cells between wt and PTX3-deficient mice.

Among the different mechanisms influencing granulation tissue formation, cell locomotion and proliferation into the ECM appear to play a major role (Clark, 2001; Singer and Clark, 1999). On invasion and digestion of the provisional scaffold of fibrin, remodeling cells lay down a collagen-rich matrix that contributes to further granulation tissue maturation (Romer et al., 1996). MSCs are key elements of granulation tissue (McClain et al., 1996), can be attracted by paracrine signals, and, together with fibroblasts and epidermal cells, favor the provisional fibrin-matrix remodeling (Agis et al., 2009; Neuss et al., 2010). Our findings, showing impaired wound closure as early as 2 days after administration of *Ptx3*$^{-/-}$ MSCs to the injury site, seem to indicate that PTX3 affects MSC functions in the early phases of wound healing. In this regard, as previously shown for Ptx3-deficient cells during tissue remodeling (Doni et al., 2015), at day 2 after wounding, *Ptx3*$^{-/-}$ MSCs failed to be recruited to the wound site and displayed a defective invasive phenotype associated with an impaired therapeutic effect. Because early delivery of MSCs at the site of injury is crucial to achieve optimal repair and/or regeneration (Chen et al., 2008), we hypothesize that a limited amount of engrafted *Ptx3*$^{-/-}$ MSCs might have been the cause of the delayed wound closure observed in our specimens.

Furthermore, in keeping with data showing an interaction between PTX3, fibrinogen and/or fibrin, and plasminogen, which favored enhanced fibrinolysis (Doni et al., 2015), we show that PTX3 deficiency in MSC treatment is associated with increased fibrin deposition and decreased levels of D-dimer versus control wounds. In this regard, our in vivo results indicate that a delay in clot remodeling indeed occurs in wounds treated with *Ptx3*$^{-/-}$ MSCs, indicating an impaired ability of these cells to digest the fibrin, which likely inhibits their ability to migrate to the injured site. The occurrence of

these events might also hamper the recruitment of other remodeling cells into the wound bed.

Consistent with these findings, pericellular fibrinolysis, in vitro, was found to be severely affected in *Ptx3*$^{-/-}$ MSCs compared with wt cells. Furthermore, fibrin digestion by MSCs was completely prevented by the presence of plasminogen-conversion inhibitors (aprotinin and plasminogen activator inhibitor-1), suggesting a plasmin-mediated fibrinolysis mechanism in our model. In support of our results in vitro, at day 2, we observed colocalization of PTX3 and fibrin into the wound and in the pericellular matrix of wt MSCs. Thus, it is likely that, in the earlier phases of wound healing, the secretion of PTX3 around MSCs and in the injured tissue creates, through fibrin digestion, an environment that fosters the recruitment of MSCs and other circulating cells. Experiments are under way to determine whether restoring PTX3 expression in *Ptx3*$^{-/-}$ MSCs can rescue MSCs-mediated fibrinolysis in vitro.

Finally, several studies have shown that the chemokine CXCL12 is critical for stem and/or progenitor and mesenchymal cell homing in injured tissues through interaction with its cognate receptor CXCR4 (Liu et al., 2011; Son et al., 2006). Here, we show that migration of *Ptx3*$^{-/-}$ MSCs in response to CXCL12 is significantly reduced through the fibrin layer, providing further evidence that poor invasion of fibrin may be the rate-limiting step in MSC movement through the wound.

Thus, taken all together, our results suggest that the fibrinolysis mediated by MSC-derived PTX3 is directly related to the dissolution of clot and fibrin-rich provisional matrix remodeling required for the migration of these cells into the wound, which constitutes an important prerequisite for appropriate wound healing in our model. Moreover, it is likely that, by creating passages into the fibrin clot, the invading MSCs may promote the recruitment of other remodeling cells, thereby favoring the acceleration of repair processes such as granulation tissue maturation.

Overall, our findings support a model where PTX3 acts as a potent promoter of tissue repair and/or remodeling exerted by MSCs and provide further evidence of a potential therapeutic approach for nonhealing wounds.

MATERIALS AND METHODS

Additional techniques are available in the supplementary material online.

MSC isolation

wt and *Ptx3*$^{-/-}$ MSCs were obtained from the BM of C57BL6/J wt and *Ptx3*$^{-/-}$ mice, respectively. Mononuclear cells were isolated using Ficoll-Paque PLUS (GE Healthcare, Little Chalfont, UK) and seeded at 16 $\times$ 10^4 cells/cm^2 in low glucose Dulbecco's Modified Eagle Medium (Lonza, Verviers, Belgium) supplemented with 20% fetal bovine serum (Biosera, Ringmer, UK) at 37 °C with 5% CO_2. After 24–48 hours, nonadherent cells were removed and adherent cells were allowed to reach 70–80% confluence. MSCs were used between passages 5 and 8.

GFP$^+$ MSCs were generated through plasmid murine stem cell virus-internal ribosomal entry site-GFP-mediated infection (Pear et al., 1998). After 72 hours, MSCs were detached and the levels of GFP were evaluated by FACS analysis. The percentage of infected GFP$^+$ cells was found to range from 94% to 96% in both MSC lines.

Animals

wt and *Ptx3*$^{-/-}$ mice, 8–12 weeks of age, were purchased from Charles River Laboratories (Milan, Italy) and housed in individual, ventilated, and pathogen-free cages of conventional animal facility in the Milano-Bicocca University. Procedures involving animal handling and care were conformed to protocols approved by the Milano-Bicocca University in compliance with national and international law and policies. This study was approved by the Italian Ministry of Health (approval no. 9/2011-B, issued on 19 January 2011).

Wound healing model

A full-thickness wound was created on anesthetized 129/Sv mice (2.5% Avertin, Sigma-Aldrich, St. Louis, MO) with a sterile 8-mm-diameter biopsy punch by excising the skin and the underlying panniculus carnosus. A total of 10^6 *Ptx3*$^{-/-}$ or wt MSCs were immediately transplanted via injection and topical administration. Briefly, 0.7 $\times$ 10^6 MSCs were subcutaneously injected around the wound (four injections) and 0.3 $\times$ 10^6 MSCs were applied onto the wound bed. Phosphate buffered saline and growth factor reduced Matrigel (BD, Bedford, MA) were used as vehicles, respectively. Wounds were daily photographed and measured by tracing the margins onto a transparent film. The areas were obtained using ImageJ software (version 1.44x, NIH, Bethesda, MD), and the rate of wound closure was calculated as the ratio of the area at each time point to the area at time 0 (immediately after wounding).

Pericellular fibrinolysis

wt or *Ptx3*$^{-/-}$ MSCs (3 $\times$ 10^3/ml) were suspended in a mixture of 2.5 mg/ml plasminogen-free fibrinogen (Sigma-Aldrich). Thrombin (1 U/ml) (Sigma-Aldrich) was then added and the suspension immediately poured into a 24-multiwell plate on rounded glasses. The plate was incubated for 30 minutes at 37 °C to allow fibrin polymerization. After washing with PBS^{2+}, fibrin cultures were incubated with complete Dulbecco's Modified Eagle Medium in triplicate at 37 °C. For inhibitory studies (100 kU/ml), aprotinin or (1 μg/ml) plasminogen activator inhibitor-1 (Calbiochem-Merck, Frankfurt, Germany) was added to the cultures. Fibrinolysis was evaluated after 36 hours by quantifying fibrinolysis-derived products released in the culture medium by ELISA and Western blot. Purified rabbit polyclonal antibody antifibrinogen (500 ng/ml; Dako, Glostrup, Denmark) was used to detect the soluble fibrinolysis-derived products.

Statistical analysis

Results are expressed as mean ± SEM. Statistical significance between groups was assessed by unpaired two-tailed Student's *t* or Mann-Whitney test with Prism software (version 4.00 for Windows; GraphPad, Inc, La Jolla, San Diego, CA).

CONFLICT OF INTEREST

The authors state no conflict of interest.

ACKNOWLEDGMENTS

This work has been partly supported by grants from Associazione Italiana Ricerca sul Cancro (AIRC 5X1000 and AIRC to GD'A) and by Italian Ministry of Health. The authors would like to thank "Fondazione Matilde Tettamanti," "Comitato Maria Letizia Verga," and "Comitato Stefano Verri" for their generous and continuous support.

SUPPLEMENTARY MATERIAL

Supplementary material is linked to the online version of the article at www.jidonline.org, and at http://dx.doi.org/10.1038/JID.2015.346.

REFERENCES

Agis H, Kandler B, Fischer MB, Watzek G, Gruber R. Activated platelets increase fibrinolysis of mesenchymal progenitor cells. J Orthop Res 2009;27:972–80.

Alfaro MP, Pagni M, Vincent A, et al. The Wnt modulator sFRP2 enhances mesenchymal stem cell engraftment, granulation tissue formation and myocardial repair. Proc Natl Acad Sci USA 2008;105:18366–71.

Badiavas EV, Abedi M, Butmarc J, Falanga V, Quesenberry P. Participation of bone marrow derived cells in cutaneous wound healing. J Cell Physiol 2003;196:245–50.

Bey E, Prat M, Duhamel P, et al. Emerging therapy for improving wound repair of severe radiation burns using local bone marrow-derived stem cell administrations. Wound Repair Regen 2010;18:50–8.

Bottazzi B, Doni A, Garlanda C, Mantovani A. An integrated view of humoral innate immunity: pentraxins as a paradigm. Annu Rev Immunol 2010;28:157–83.

Carmeliet P, Schoonjans L, Kieckens L, et al. Physiological consequences of loss of plasminogen activator gene function in mice. Nature 1994;368:419–24.

Chen L, Tredget EE, Wu PY, Wu Y. Paracrine factors of mesenchymal stem cells recruit macrophages and endothelial lineage cells and enhance wound healing. PloS One 2008;3:e1886.

Chiellini C, Cochet O, Negroni L, et al. Characterization of human mesenchymal stem cell secretome at early steps of adipocyte and osteoblast differentiation. BMC Mol Biol 2008;9:26.

Ciccocioppo R, Bernardo ME, Sgarella A, et al. Autologous bone marrow-derived mesenchymal stromal cells in the treatment of fistulising Crohn's disease. Gut 2011;60:788–98.

Clark RA. Fibrin and wound healing. Ann N Y Acad Sci 2001;936:355–67.

de Giorgio-Miller A, Bottoms S, Laurent G, Carmeliet P, Herrick S. Fibrin-induced skin fibrosis in mice deficient in tissue plasminogen activator. Am J Pathol 2005;167:721–32.

Deban L, Russo RC, Sironi M, et al. Regulation of leukocyte recruitment by the long pentraxin PTX3. Nat Immunol 2010;11:328–34.

Dinarello CA. Immunological and inflammatory functions of the interleukin-1 family. Annu Rev Immunol 2009;27:519–50.

Doni A, Musso T, Morone D, et al. An acidic microenvironment sets the humoral pattern recognition molecule PTX3 in a tissue repair mode. J Exp Med 2015;212:905–25.

Falanga V, Iwamoto S, Chartier M, et al. Autologous bone marrow-derived cultured mesenchymal stem cells delivered in a fibrin spray accelerate healing in murine and human cutaneous wounds. Tissue Eng 2007;13:1299–312.

Hocking AM, Gibran NS. Mesenchymal stem cells: paracrine signaling and differentiation during cutaneous wound repair. Exp Cell Res 2010;316:2213–9.

Javazon EH, Keswani SG, Badillo AT, et al. Enhanced epithelial gap closure and increased angiogenesis in wounds of diabetic mice treated with adult murine bone marrow stromal progenitor cells. Wound Repair Regen 2007;15:350–9.

Liu S, Jiang L, Li H, et al. Mesenchymal stem cells prevent hypertrophic scar formation via inflammatory regulation when undergoing apoptosis. J Invest Dermatol 2014;134:2648–57.

Liu X, Duan B, Cheng Z, et al. SDF-1/CXCR4 axis modulates bone marrow mesenchymal stem cell apoptosis, migration and cytokine secretion. Protein Cell 2011;2:845–54.

Lu J, Marnell LL, Marjon KD, Mold C, Du Clos TW, Sun PD. Structural recognition and functional activation of FcgammaR by innate pentraxins. Nature 2008;456:989–92.

Martin P. Wound healing—aiming for perfect skin regeneration. Science 1997;276:75–81.

McClain SA, Simon M, Jones E, et al. Mesenchymal cell activation is the rate-limiting step of granulation tissue induction. Am J Pathol 1996;149:1257–70.

McFarlin K, Gao X, Liu YB, et al. Bone marrow-derived mesenchymal stromal cells accelerate wound healing in the rat. Wound Repair Regen 2006;14:471–8.

Medzhitov R. Origin and physiological roles of inflammation. Nature 2008;454:428–35.

Neuss S, Schneider RK, Tietze L, Knüchel R, Jahnen-Dechent W. Secretion of fibrinolytic enzymes facilitates human mesenchymal stem cell invasion into fibrin clots. Cells Tissues Organs 2010;191:36–46.

Norata GD, Marchesi P, Pulakazhi Venu VK, et al. Deficiency of the long pentraxin PTX3 promotes vascular inflammation and atherosclerosis. Circulation 2009;120:699–708.

Pear WS, Miller JP, Xu L, et al. Efficient and rapid induction of a chronic myelogenous leukemia-like myeloproliferative disease in mice receiving P210 bcr/abl-transduced bone marrow. Blood 1998;92:3780–92.

Rodriguez-Grande B, Swana M, Nguyen L, et al. The acute-phase protein PTX3 is an essential mediator of glial scar formation and resolution of brain edema after ischemic injury. J Cereb Blood Flow Metab 2014;34:480–8.

Romer J, Bugge TH, Pyke C, et al. Impaired wound healing in mice with a disrupted plasminogen gene. Nat Med 1996;2:287–92.

Salio M, Chimenti S, De Angelis N, et al. Cardioprotective function of the long pentraxin PTX3 in acute myocardial infarction. Circulation 2008;117:1055–64.

Sasaki M, Abe R, Fujita Y, Ando S, Inokuma D, Shimizu H. Mesenchymal stem cells are recruited into wounded skin and contribute to wound repair by transdifferentiation into multiple skin cell type. J Immunol 2008;180:2581–7.

Sellheyer K, Krahl D. Skin mesenchymal stem cells: prospects for clinical dermatology. J Am Acad Dermatol 2010;63:859–65.

Singer AJ, Clark RA. Cutaneous wound healing. N Engl J Med 1999;341:738–46.

Son BR, Marquez-Curtis LA, Kucia M, et al. Migration of bone marrow and cord blood mesenchymal stem cells in vitro is regulated by stromal-derived factor-1-CXCR4 and hepatocyte growth factor-c-met axes and involves matrix metalloproteinases. Stem Cells 2006;24:1254–64.

Toma JG, Akhavan M, Fernandes KJ, et al. Isolation of multipotent adult stem cells from the dermis of mammalian skin. Nat Cell Biol 2001;3:778–84.

Wu Y, Chen L, Scott PG, Tredget EE. Mesenchymal stem cells enhance wound healing through differentiation and angiogenesis. Stem Cells 2007;25:2648–59.